AMERICAN SOCIETY FOR MICROBIOLOGY | Journal of Bacteriology®

RESEARCH ARTICLE

Fine-Tuning of σ^E Activation Suppresses Multiple Assembly-Defective Mutations in *Escherichia coli*

Elizabeth M. Hart,[a] Aileen O'Connell,[a,b] Kimberly Tang,[a] Joseph S. Wzorek,[c,d] Marcin Grabowicz,[a,e,f,g] Daniel Kahne,[c] Thomas J. Silhavy[a]

[a]Department of Molecular Biology, Princeton University, Princeton, New Jersey, USA
[b]Laboratory of Virology and Infectious Disease, The Rockefeller University, New York, New York, USA
[c]Department of Chemistry and Chemical Biology, Harvard University, Cambridge, Massachusetts, USA
[d]Novartis Institute for BioMedical Research, Inc., Cambridge, Massachusetts, USA
[e]Emory Antibiotic Resistance Center, Emory University School of Medicine, Atlanta, Georgia, USA
[f]Department of Microbiology and Immunology, Emory University School of Medicine, Atlanta, Georgia, USA
[g]Division of Infectious Disease, Department of Medicine, Emory University School of Medicine, Atlanta, Georgia, USA

ABSTRACT The Gram-negative outer membrane (OM) is a selectively permeable asymmetric bilayer that allows vital nutrients to diffuse into the cell but prevents toxins and hydrophobic molecules from entering. Functionally and structurally diverse β-barrel outer membrane proteins (OMPs) build and maintain the permeability barrier, making the assembly of OMPs crucial for cell viability. In this work, we characterize an assembly-defective mutant of the maltoporin LamB, LamB^{G439D}. We show that the folding defect of LamB^{G439D} results in an accumulation of unfolded substrate that is toxic to the cell when the periplasmic protease DegP is removed. Selection for suppressors of this toxicity identified the novel mutant *degS*$_{A323E}$ allele. The mutant DegS^{A323E} protein contains an amino acid substitution at the PDZ/protease domain interface that results in a partially activated conformation of this protein. This activation increases basal levels of downstream σ^E stress response signaling. Furthermore, the enhanced σ^E activity of DegS^{A323E} suppresses a number of other assembly-defective conditions without exhibiting the toxicity associated with high levels of σ^E activity. We propose that the increased basal levels of σ^E signaling primes the cell to respond to envelope stress before OMP assembly defects threaten cell viability. This finding addresses the importance of envelope stress responses in monitoring the OMP assembly process and underpins the critical balance between envelope defects and stress response activation.

IMPORTANCE Gram-negative bacteria, such as *Escherichia coli*, inhabit a natural environment that is prone to flux. In order to cope with shifting growth conditions and the changing availability of nutrients, cells must be capable of quickly responding to stress. Stress response pathways allow cells to rapidly shift gene expression profiles to ensure survival in this unpredictable environment. Here we describe a mutant that partially activates the σ^E stress response pathway. The elevated basal level of this stress response allows the cell to quickly respond to overwhelming stress to ensure cell survival.

KEYWORDS DegS, envelope stress responses, LamB, outer membrane, outer membrane proteins, protease, sigma E

The outer membrane (OM) of Gram-negative bacteria functions as a robust permeability barrier that selectively allows nutrients into the cell but prevents harmful molecules, such as antibiotics, from entering. Due to this critical balance, the biogenesis of the OM is a precisely regulated process that is essential for cell viability. The main

Citation Hart EM, O'Connell A, Tang K, Wzorek JS, Grabowicz M, Kahne D, Silhavy TJ. 2019. Fine-tuning of σ^E activation suppresses multiple assembly-defective mutations in *Escherichia coli*. J Bacteriol 201:e00745-18. https://doi.org/10.1128/JB.00745-18.

Editor George O'Toole, Geisel School of Medicine at Dartmouth

Address correspondence to Thomas J. Silhavy, tsilhavy@princeton.edu.

For a companion article on this topic, see https://doi.org/10.1128/JB.00742-18.

Received 30 November 2018
Accepted 25 February 2019
Accepted manuscript posted online 11 March 2019
Published 8 May 2019

functions of the OM, namely, the passage of nutrients, the efflux of toxins, and the maintenance of membrane integrity, are carried out by integral β-barrel outer membrane proteins (OMPs). Consequently, defects in OMP assembly disrupt the selectivity of the permeability barrier and leave the cell vulnerable to antibiotics and other environmental threats (1, 2).

The early stages of the OMP assembly pathway have been extensively characterized over the past 5 decades. Briefly, precursor OMPs are transported across the inner membrane (IM) by the Sec translocon (3, 4). Chaperones, such as SurA, bind the OMP at the periplasmic face of the IM and ferry the processed, mature protein across the periplasm to the OM. During transport, SurA maintains the OMP in an unfolded state in order to prevent aggregation and misfolding in the oxidizing environment of the periplasm. The unfolded OMP is delivered to the heteropentomeric β-barrel assembly machine (Bam complex) and is assembled into the OM (5, 6). The mechanism by which the Bam complex interacts with and folds OMPs remains poorly understood.

Folding defects, translational error, or conditions that disrupt protein assembly can result in OMPs falling off the assembly pathway and misfolding in the periplasm. Unchecked, this accumulation of unfolded proteins will lead to cell death (7, 8). The σ^E stress response monitors the cell for toxic aggregates and alters gene expression in response. In wild-type cells, OMP assembly is incredibly efficient and unfolded OMPs cannot be detected at steady-state levels (9, 10).

The σ^E pathway detects periplasmic stress input and initiates a proteolytic cascade that results in the sequential degradation of the anti-sigma factor RseA (10). Unfolded OMPs bind the essential IM protease DegS and activate cleavage of the periplasmic domain of RseA (11–13). This stimulates degradation of the inner membrane region of RseA by RseP, resulting in the release of the cytoplasmic domain of the anti-sigma factor (14–17). The σ^E-bound cytoplasmic domain is then cleaved by ClpXP, freeing σ^E to transcribe its regulon (18–20). Included in the regulon are Bam complex members, chaperones, proteases, and small RNAs to repress expression of OMPs, among others (21, 22). Thus, activation of the σ^E response shifts the gene expression profile to improve the transport and assembly of OMPs, enhance the degradation of unfolded proteins that have aggregated in the periplasm, and slow the influx of precursor OMPs into the assembly pathway.

Regulation of the σ^E stress response pathway is critical to cell viability (23, 24). Constitutive activation of σ^E in the absence of stress, such as in the case of *rseA* null mutations, causes growth defects under standard culturing conditions (19, 25–28). The cell maintains control over σ^E activity through translational regulation; ribosomal profiling studies show that translation rates of RseA are much higher than those of σ^E (29, 30). The ability of the cell to turn the σ^E pathway on in the presence of stress, shut it off when the threat subsides, and prevent activation in the absence of stress, is critical to cell survival (12, 24).

Here we characterize an assembly-defective mutant of the maltoporin LamB that accumulates as an unfolded OMP substrate that is toxic under certain conditions. Selection for suppressors identified a novel mutation that alters the IM protease DegS and partially activates the σ^E stress response. This mutation also suppresses other distinct assembly-defective mutations, suggesting that the fine-tuning of σ^E activity may have a significant impact on cell viability in otherwise toxic backgrounds.

RESULTS

LamB^{G439D} is an assembly-defective mutant. To investigate critical interactions that take place during OMP biogenesis, we perturbed the assembly process with a defective OMP substrate. We selected the maltoporin LamB as a candidate protein due to the ability to assay LamB assembly through maltodextrin utilization (31, 32). To impair assembly of LamB, we performed site-directed mutagenesis on a plasmid-encoded *lamB* under the control of a tetracycline-inducible promoter in order to avoid feedback from maltodextrin intake on the native promoter and assayed function in strains in which the native copy of *lamB* was deleted (33, 34). We selected a C-terminal

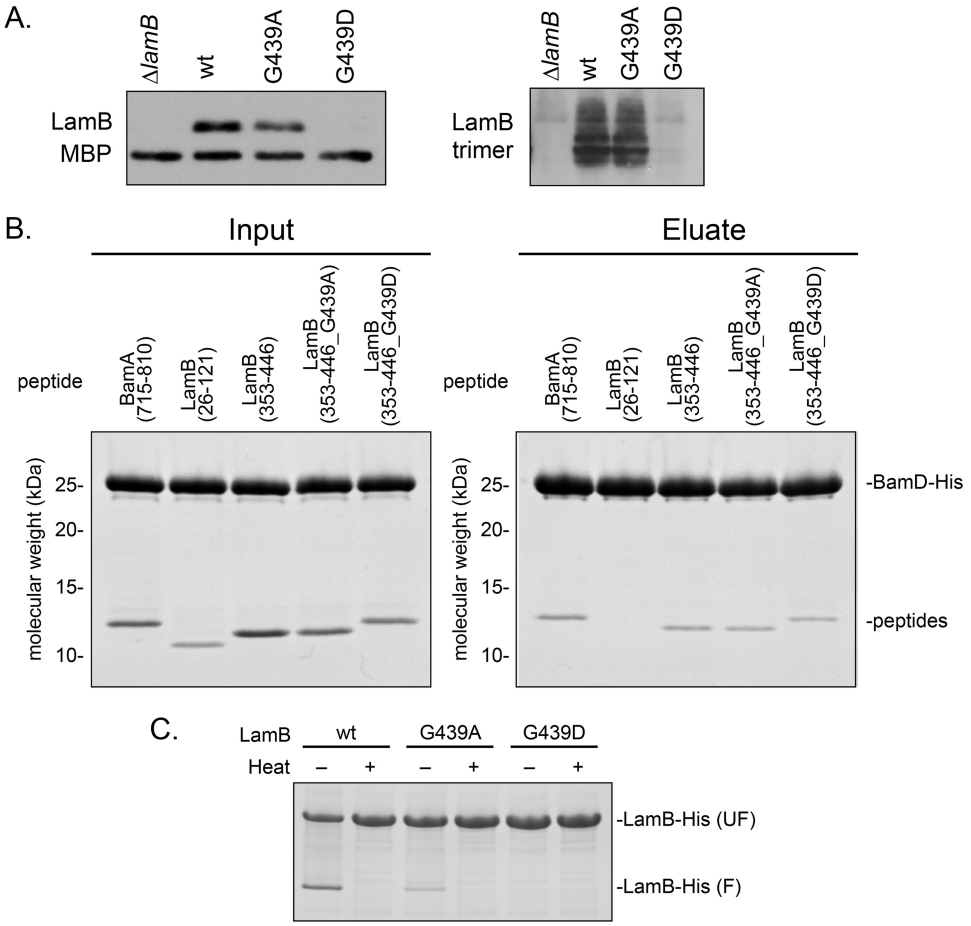

FIG 1 LamB^{G439D} is a folding-defective mutant. (A) Monomeric and trimeric LamB levels were determined in strains with the genotypes listed by SDS-PAGE and immunoblotting. Antibodies specific to the monomeric and trimer protein were used. (B) Purified LamB peptides were incubated with His-tagged BamD and coimmunoprecipitated and analyzed by SDS-PAGE analysis. (C) Purified LamB protein was boiled (denatured) or incubated at room temperature (nondenatured) and examined by electrophoresis.

conserved glycine at residue 439 for mutagenesis, as mutations of similarly positioned glycine residues have been shown to impair assembly of other OMPs (35–38). Residue G439 was mutated to alanine or a charge was introduced with an aspartate. To examine the effect of these mutations on LamB assembly, we assayed levels of monomeric and functional trimeric protein in cells grown at 30°C (Fig. 1A). Cells expressing *lamB*$_{G439A}$ showed similar levels of monomeric and trimeric LamB as a control strain expressing wild-type *lamB*, whereas cells expressing *lamB*$_{G439D}$ exhibited drastically reduced levels of both forms of LamB. However, cells expressing *lamB*$_{G439D}$ formed red colonies on MacConkey maltodextrin agar (see Fig. S1 in the supplemental material) and were able to grow in defined minimal maltodextrin medium (Table S1), indicating that there was a small amount of functional protein assembled into the OM. We concluded that LamB^{G439D}, and not LamB^{G439A}, was assembly defective; however, it remained unclear at what stage of assembly LamB^{G439D} was impaired.

We hypothesized that the charge substitution could interfere with interactions with the Bam complex or with folding, as other previously described assembly-defective substrates exhibit defects at these stages in assembly (37–40). To determine if LamB^{G439D} interacts aberrantly with the Bam complex, we measured the binding of LamB peptides encompassing residue 439 to the Bam complex using affinity copurification (Fig. 1B). We used binding to BamD as a measure of Bam complex engagement with the mutant substrate due to the role of BamD in recognizing OMPs (37, 39, 41). We first confirmed that residue 439 was located in a region of the protein that interacts

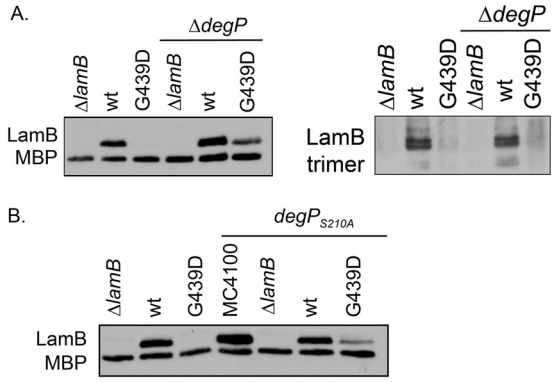

FIG 2 The absence of DegP protease function stabilizes monomeric LamB^{G439D} at 30°C. Monomeric or trimeric LamB was detected using whole-cell lysates made from strains of the listed genotypes, in Δ*degP* or *degP*$_{S210A}$ *yadC*::Tn*10* backgrounds, and analyzed by SDS-PAGE and immunoblotting. Antibodies that specifically detect monomeric and trimer LamB were used.

with the Bam complex. LamB peptides encompassing residues 353 to 446 were able to bind BamD, while peptides comprised of residues 26 to 121 did not copurify with BamD, indicating that the protein region surrounding residue 439 binds to the Bam complex. Furthermore, we determined that LamB peptides (residues 353 to 446) containing G439A and G439D mutations bound to His-tagged BamD similarly to the wild-type peptide, indicating that neither mutation changes the ability of LamB to engage with the Bam complex.

β-Barrel proteins are resistant to denaturation by SDS alone, allowing the folding status of the protein to be assayed by comparing heat-denatured and nondenatured (incubated at room temperature) samples, a property called heat modifiability (42). Figure 1C shows heat modifiability of purified LamB following an *in vitro* folding assay. Purified wild-type LamB and LamB^{G439A} are folding competent under nondenaturing conditions, evidenced by the appearance of folded molecules in nondenatured samples. However, no amount of folded LamB^{G439D} could be detected in the nondenatured samples. We conclude that LamB^{G439D} is an assembly-defective mutant that is impaired in folding but not in recognition by the Bam complex.

Unfolded LamB^{G439D} is toxic in the absence of *degP*. Often, mutant OMP substrates fall off the assembly pathway and misfold in the periplasm. Periplasmic proteases degrade the misfolded protein to prevent the toxicity associated with the accumulation of unfolded proteins (7, 8, 43). The folding defect of LamB^{G439D}, then, may make the assembly-defective protein a substrate of the periplasmic protease DegP. To examine this possibility, we deleted *degP* and monitored levels of monomeric and trimeric LamB^{G439D} in cells grown at 30°C (Fig. 2A). Deletion of *degP* restored whole-cell monomeric protein levels, supporting the model that LamB^{G439D} accumulates in the periplasm and is degraded by DegP. However, very little of the stabilized monomeric LamB^{G439D} is assembled into the OM, as evidenced by the minimal increase in functional LamB^{G439D} trimers (Fig. 2A). The red colony phenotype on MacConkey maltodextrin agar and ability to grow in minimal maltodextrin media indicate that Δ*degP* *lamB*$_{G439D}$ cells do have functional LamB^{G439D} in the OM (Fig. S1 and Table S1). A protease-null mutant of *degP*, *degP*$_{S210A}$, also stabilizes levels of monomeric LamB^{G439D} (Fig. 2B) (44). Thus, the absence of the DegP protease function stabilizes unfolded LamB^{G439D} monomers, but the majority of this protein is not assembled into the OM.

Intriguingly, deletion of *degP* in a *lamB*$_{G439D}$ background is lethal at 37°C. To further demonstrate this conditional synthetic phenotype, we used genetic linkage analysis to quantify the frequency at which a *degP*::*kan* allele can be moved into the *lamB*$_{G439D}$ strain at 30°C and 37°C by cotransduction with a nearby *yadC*::Tn*10* marker (Table 1). *degP*::*kan* can be moved into the *lamB*$_{G439D}$ strain at 30°C, albeit with some linkage disruption. However, the allele cannot be moved into the strain at the higher temper-

TABLE 1 *degP* deletion is synthetically lethal with $lamB_{G439D}$ at 37°C

	degP::*kan yadC*::Tn*10* cotransduction frequency (%)[a]	
Recipient strain	**30°C**	**37°C**
MC4100	50	44
Δ*lamB* strain	53	47
Δ*lamB* p$lamB^+$ strain	53	40
Δ*lamB* p$lamB_{G439D}$ strain	27	<1

[a]P1*vir* lysates carrying *degP*::*kan yadC*::Tn*10* were transduced into the indicated strains at the designated temperature. The Tet^r transductants were then tested for Kan^r to calculate cotransduction of *degP*::*kan* and *yadC*::Tn*10* markers. Cotransduction frequency represents three separate transductions.

ature, confirming that deletion of *degP* is synthetically lethal with $lamB_{G439D}$ at 37°C. We posit that the accelerated growth rate of cells at 37°C leads to a toxic aggregation of unfolded LamB^{G439D} that results in cell death.

Isolation of a suppressor of the Δ*degP* $lamB_{G439D}$ mutation. We took advantage of the synthetic lethality of $lamB_{G439D}$ with *degP* deletion at 37°C to select for suppressors that restored assembly of the defective protein. To do this, we grew Δ*degP* $lamB_{G439D}$ cells at the permissive temperature of 30°C overnight, diluted the cultures, and plated them on MacConkey maltodextrins at 37°C. This strategy allowed us to select for suppressors that allowed viability of cells at the nonpermissive temperature and to screen for those that properly assembled LamB. Assembly of LamB was assayed using growth phenotype on the MacConkey maltodextrin agar; red colony color indicates that the cell assembled LamB and was able to take in maltodextrins (Fig. S1) (45).

Most of the spontaneous suppressors restored growth at 37°C but did not restore assembly of LamB, resulting in white colonies on MacConkey maltodextrin agar. The high rate of suppressors that restored growth but not assembly of LamB suggests that they were *lamB* null mutations, and this underscores the toxicity of LamB^{G439D}. We identified a chromosomal suppressor that was viable at both 30°C and 37°C and formed red colonies on MacConkey medium supplemented with maltodextrins (Fig. 3A). Using whole-genome sequencing, we identified the $degS_{A323E}$ mutation and subsequently confirmed that this was a suppressor by marker rescue.

Immunoblot analysis showed that the suppressor mutation efficiently restored levels of trimeric LamB^{G439D} at 30°C and stabilized monomeric protein at 37°C (Fig. 3C, compare lanes 22 to 23, and Fig. 3B, compare lanes 7 to 8). The suppressor mutation increased levels of LamB, LamB^{G439D}, and OmpA at higher temperatures (Fig. 3B compare lanes 7 and 8, and lanes 13 and 14). However, it did not restore efficient trimer assembly of LamB^{G439D} (Fig. 3C). This suggests that the $degS_{A323E}$ suppressor mutation both aids in the assembly of the mutant protein and ameliorates the toxicity of LamB^{G439D} in a temperature-dependent manner.

***$degS_{A323E}$* increases basal levels of σ^E signaling.** DegS^{A323E} contains an alanine-to-glutamate substitution at residue 323, which is located at the interface between the PDZ and protease domains of the protein (Fig. 4A). Salt bridges at this interface stabilize the inactive conformation of DegS and are disrupted as a result of steric clashes upon OMP binding to the PDZ domain. Previous studies have shown that altering residues in the PDZ/protease domain interface changes the activity of DegS, likely through disruption of the salt bridge network (46–50). To assay DegS^{A323E} activity, we monitored σ^E activation through measurement of β-galactosidase activity from a σ^E-dependent *lacZ* reporter (Fig. 4B and C) (51). $degS_{A323E}$ showed increased basal levels of σ^E activity in an otherwise isogenic, wild-type strain. This increase in σ^E activity was comparable to the levels of induction observed in a Δ*surA* strain but lower than activation in an *rseA* null strain, which exhibited fully active σ^E signaling (Fig. 4B and C) (52, 53). However, $degS_{A323E}$ did prevent further induction when the σ^E response was induced. $degS_{A323E}$ Δ*surA* and $degS_{A323E}$ Δ*rseA* double mutants showed levels of σ^E activation similar to those of Δ*surA* and Δ*rseA* mutants, respectively (Fig. 4B and C). $degS_{A323E}$, then, primes

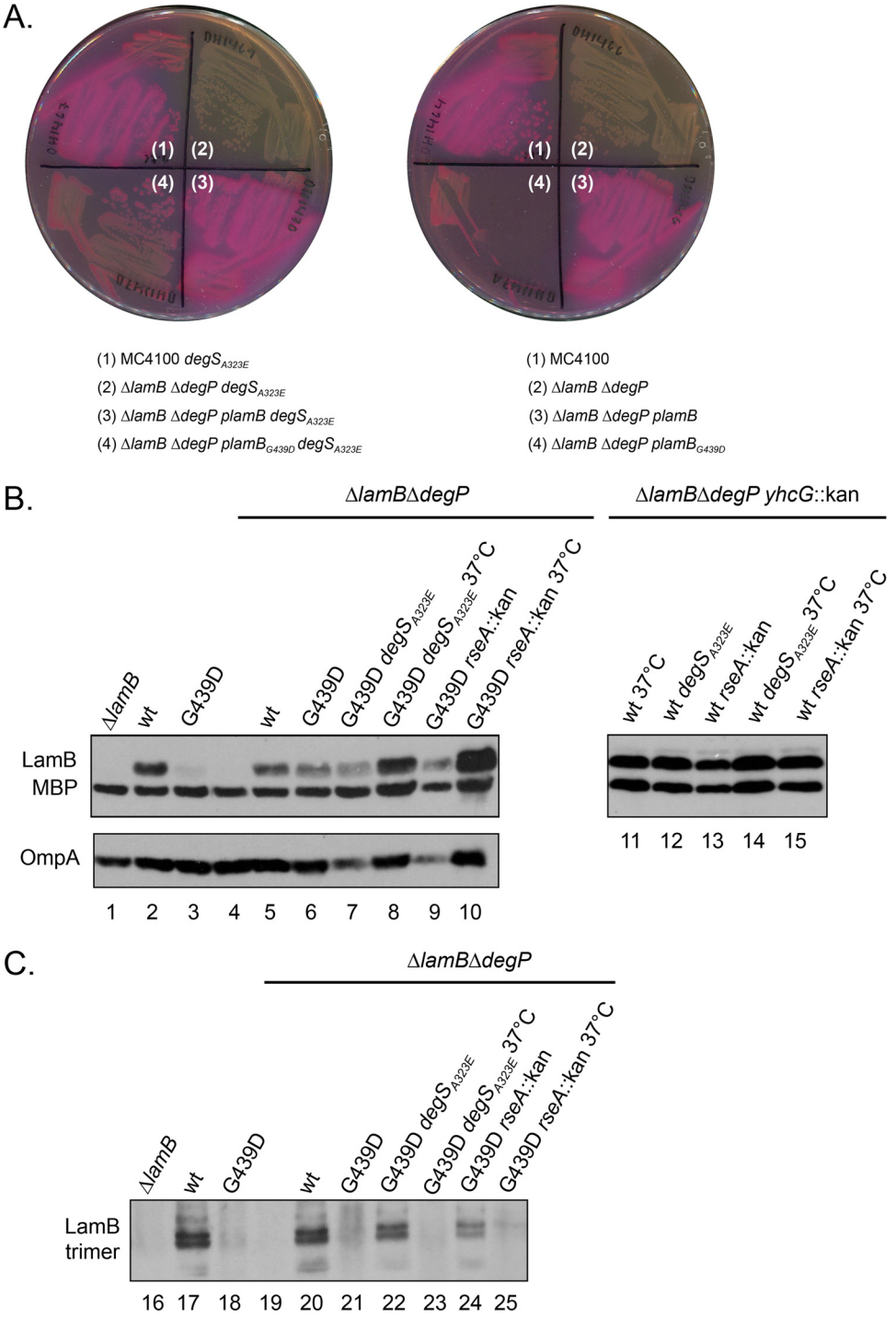

FIG 3 degS$_{A323E}$ suppresses lamB$_{G439D}$. (A) The indicated strains were streaked onto MacConkey maltodextrin indicator agar at 37°C. Strains not carrying the plasmid-borne *lamB* carry an empty vector control. (B and C) Whole-cell lysates of the indicated strains were analyzed by SDS-PAGE and immunoblotting. Monomeric and trimeric LamB was detected using antibodies specific for those protein conformations. Unless otherwise indicated, the strains were grown at 30°C.

the cell to handle stress with a higher basal level of σ^E activation, but this signaling is not further enhanced by DegS^{A323E} when stress is present.

To determine if elevated σ^E activity was sufficient for suppression, we tested if other mutations that increase levels of σ^E signaling could also suppress the Δ*degP lamB*$_{G439D}$ mutation. Deletion of the anti-sigma factor gene *rseA* phenocopied the degS$_{A323E}$

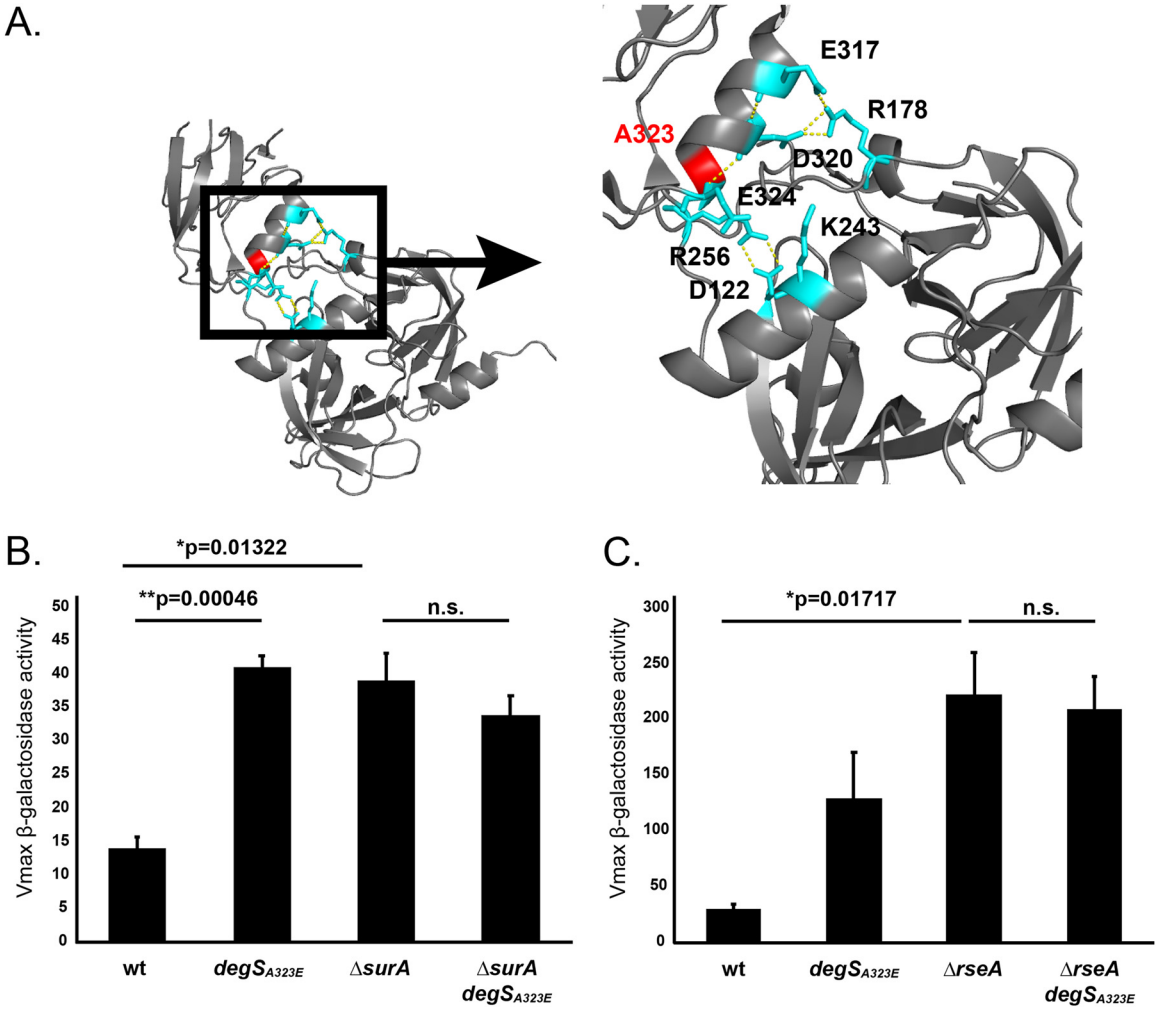

FIG 4 *degS*$_{A323E}$ partially activates basal levels of σ^E signaling. (A) DegS^{A323} (red) is located at the PDZ/protease domain interface of DegS. These domains interact by a number of salt bridges (teal) that stabilize the inactive conformation of the protein. Dashed lines indicate polar contacts. The image was generated from the peptide-free structure of DegS (PDB code 1SOT) (48). (B and C) Measurement of the V_{max} of β-galactosidase activity driven from *rpoH*P3, a σ^E-dependent promoter, in the indicated strains (51). Graphs are plotted as means ± SEM ($n = 3$). Significance was calculated using a *t* test. Strains were grown at 37°C (B) and 30°C (C). n.s., not significant.

suppressor; levels of trimeric LamB^{G439D} were more efficiently restored at 30°C and levels of the monomeric protein were stabilized at 37°C (Fig. 3B). Removal of RseA, however, impacted cell viability and prevented robust growth on MacConkey maltodextrin agar even in wild-type strains (Fig. S2). This is likely due to the toxic elevation of σ^E activity in cells lacking RseA (20, 25–28, 54).

In contrast, cells expressing *degS*$_{A323E}$ in an otherwise wild-type background grew similarly to wild-type cells at both 30°C and 37°C, indicating that the enhanced σ^E activity of this allele does not impact growth (Fig. S3). Our data show that multiple mutations that elevate σ^E activity can suppress the Δ*degP lamB*$_{G439D}$ mutation and suggest that the lowered activation of the *degS*$_{A323E}$ allele prevents the toxic effects of overactive stress signaling.

Increase in σ^E signaling by DegS^{A323E} suppresses many assembly-defective mutations. Previous studies showed that elevated σ^E activity can alleviate the phenotypes of numerous assembly-defective conditions (55, 56). Because the σ^E stress response streamlines OMP biogenesis when the cell encounters stress, we wondered if *degS*$_{A323E}$ could suppress other assembly-defective conditions. We assayed suppression of the *lptD*$_{Y721D}$ and Δ*bamB* Δ*bamE* mutations, both of which impair OMP assembly and produce outer membrane defects (Fig. 5). Importantly, *lptD*$_{Y721D}$ and Δ*bamB* Δ*bamE*

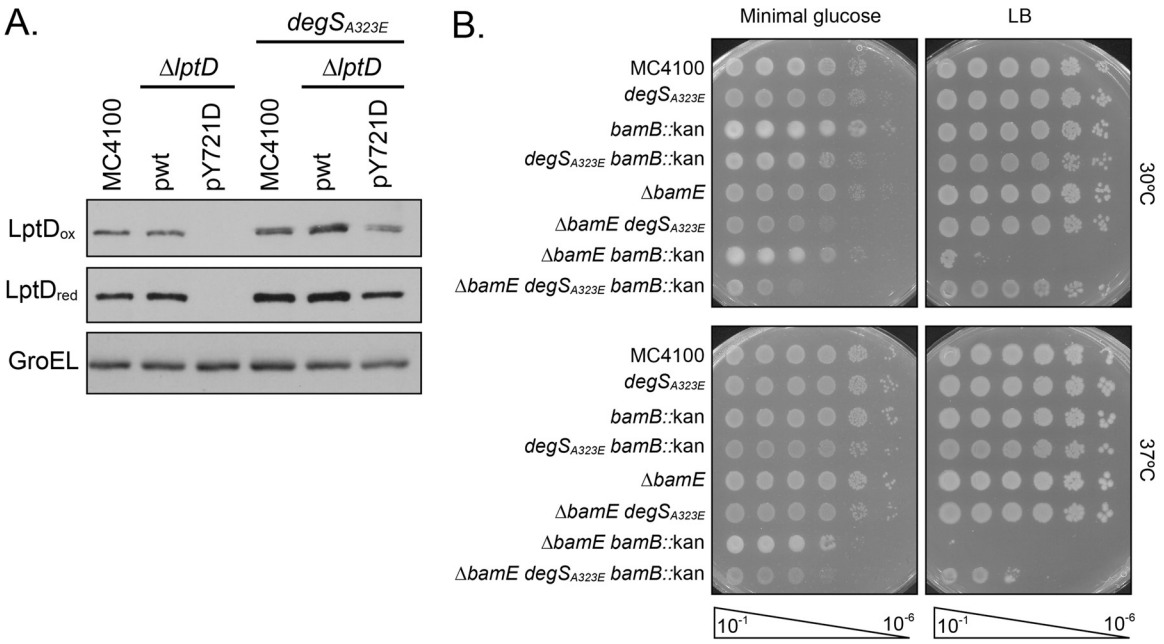

FIG 5 $degS_{A323E}$ suppresses multiple assembly-defective mutations. (A) Immunoblot analysis of whole-cell lysates to detect relative levels of LptD. Oxidized samples ("ox") were lysed with sample buffer lacking β-ME, while reduced samples ("red") were lysed with sample buffer containing β-ME. Levels of GroEL served as a loading control. (B) An efficiency-of-plating assay was performed by spotting 10-fold dilutions of overnight cultures onto LB and minimal glucose plates. Plates were incubated at the indicated temperature.

mutants are defective at distinct stages of OMP assembly, allowing us to examine the scope of $degS_{A323E}$ suppression.

$lptD_{Y721D}$ encodes an assembly-defective mutant of LptD, the OM insertase of lipopolysaccharides, that exhibits an early folding defect and stalls on BamD during assembly. Due to the deficient interaction with BamD, $LptD^{Y721D}$ falls off the assembly pathway and is degraded in the periplasm. Consequently, $lptD_{Y721D}$ is characterized by reduced levels of folded LptD protein (40, 43). We hypothesized that increasing basal levels of σ^E signaling may alleviate this phenotype. We used Western blot analysis to detect reduced and oxidized LptD, representing unfolded and folded protein, respectively, in cells expressing both $degS_{A323E}$ and $lptD_{Y721D}$ (Fig. 5A). We found that $degS_{A323E}$ increased levels of oxidized $LptD^{Y721D}$, indicating that more protein is assembled into the OM. This result shows that $degS_{A323E}$ suppresses multiple assembly-defective OMPs that are impaired at different stages of assembly.

The Δ*bamB* Δ*bamE* mutation is a conditionally lethal deletion of two lipoproteins in the Bam complex that results in global defects in OMP assembly. The drastic reduction in OMPs prevents growth of Δ*bamB* Δ*bamE* cells on rich media and at higher temperatures (57, 58). To determine if $degS_{A323E}$ could overcome a Bam complex mutant that impacts universal OMP assembly, we assayed growth of Δ*bamB* Δ*bamE* cells under nonpermissive conditions (Fig. 5B). In agreement with earlier studies, the Δ*bamB* Δ*bamE* double mutant grew only on minimal medium. $degS_{A323E}$ suppressed this growth defect and restored the ability of Δ*bamB* Δ*bamE* cells to grow on rich medium at higher temperatures. Taken together, our data show that $degS_{A323E}$ is a powerful suppressor of several conditions that weaken the OM, including assembly-defective OMP substrates and Bam complex mutations.

DISCUSSION

In this paper, we characterize the $degS_{A323E}$ mutation, a novel mutation in the σ^E stress response pathway. This mutant was isolated as a suppressor of $lamB_{G439D}$, which specifies an assembly-defective mutant of the maltoporin LamB, also described here. $LamB^{G439D}$ exhibits a folding defect that prevents robust assembly of functional protein

into the OM. We show that deletion of *degP* stabilizes monomeric LamB^{G439D} at 30°C but is synthetically lethal with *lamB*$_{G439D}$ at 37°C, suggesting that unfolded monomeric protein accumulates in the absence of the protease (Fig. 2A; Table 1). Removal of DegP only nominally increases levels of trimeric LamB^{G439D}, indicating that the majority of the monomeric protein that is stabilized in the absence of the protease is not assembled into the OM (Fig. 2A).

We isolated *degS*$_{A323E}$ as a suppressor of the Δ*degP lamB*$_{G439D}$ mutation that allowed both viability at the nonpermissive temperature and formation of red colonies on MacConkey maltodextrin agar (Fig. 3A). We have shown that *degS*$_{A323E}$ increases basal levels of σ^E activation in otherwise wild-type strains without causing growth defects (Fig. 4B; see Fig. S3 in the supplemental material). The partial σ^E activation exhibited by *degS*$_{A323E}$ is critical for viability; deletion of the anti-sigma factor gene *rseA* prevents robust growth on MacConkey agar containing maltodextrins (Fig. S2). Strikingly, *degS*$_{A323E}$ also suppresses the assembly-defective mutations *lptD*$_{Y721D}$ and the conditional lethal phenotype of a Δ*bamB* Δ*bamE* double deletion strain (Fig. 5). The partial activation of the σ^E stress response by *degS*$_{A323E}$ alleviated defects of these distinct assembly-defective conditions without creating toxicity associated with constitutively active σ^E activity.

We do not yet know the σ^E regulon member(s) directly responsible for the suppression of the Δ*degP lamB*$_{G439D}$ mutation. At 30°C, the *degS*$_{A323E}$ suppressor mutation allows efficient assembly of functional LamB^{G439D} trimers. At elevated temperatures, however, the suppressor mutation stabilizes monomeric LamB^{G439D} but does not allow efficient assembly of this protein into the OM (Fig. 3B and C). Thus, *degS*$_{A323E}$ is able to both aid assembly of the mutant protein and ameliorate the toxicity of the unfolded protein. We believe that *degS*$_{A323E}$ fine-tunes the protein quality control network to achieve the balance between stabilization of unfolded protein and assembly into the OM. The increase in σ^E signaling in cells expressing *degS*$_{A323E}$ may result in changes in the expression of both proteases and chaperones. We think it is likely that even in the presence of *degS*$_{A323E}$, assembly of LamB^{G439D} does not occur at wild-type rates. At elevated temperatures, increased growth rates increase the load on the Bam complex and assembly of LamB^{G439D} is further compromised. It is not yet clear where the mutant protein is located in the cell, but it must be sequestered in some way that its toxicity is relieved. Identifying the key σ^E regulon members induced by *degS*$_{A323E}$ and the mechanism by which this shift in gene expression profile allows for enhanced assembly or reduced toxicity in the absence of assembly will require further study.

DegS forms a homotrimer, with each monomer comprised of a protease domain and a PDZ domain that binds unfolded OMPs. Under noninducing conditions, DegS is maintained in an inactive state through autoinhibitory salt bridges at the PDZ/protease domain interface. Residues that are important for these stabilizing salt bridges include E317/R178, D320/R178, E324/K243, and D122/R256. Binding of an OMP causes a steric clash at the PDZ/protease domain interface, forcing conformational rearrangements that promote DegS activity through alignment of the catalytic triad (48–50, 59). Previously, it was shown that mutations that disrupt the autoinhibitory salt bridges or deletion of the PDZ domain altogether increases the basal activity of DegS (13, 46, 48, 50).

Residue 323 is located at the PDZ/protease domain interface and is directly adjacent to a residue that forms one of the stabilizing salt bridges that maintain the inactive conformation of the protein (D324) (48, 49). Substitution of a charged glutamate at this residue likely influences the salt bridge network that stabilizes the inactive protein in the wild-type protein. We found that DegS^{A323E} exhibits increased basal levels of σ^E signaling, suggesting that this amino acid change disrupts preexisting salt bridges to bias the protein toward the active conformation. The increase in signaling was similar to that found in *surA* null strains. DegS^{A323E} is not fully activated, as evidenced by the reduced σ^E signaling compared to an *rseA* null mutant (Fig. 4B). Thus, we believe that the system of salt bridges across the PDZ/protease domain interface is not disrupted, but rather the local network is weakened (46, 50).

degS$_{A323E}$, however, does not increase σ^E signaling under inducing conditions. We

show that the degrees of σ^E activation are equivalent in Δ*surA* and Δ*surA* $degS_{A323E}$ strains. The levels of σ^E signaling in Δ*rseA* and Δ*rseA* $degS_{A323E}$ mutants are also comparable (Fig. 4B). This is in agreement with an earlier study that shows that mutations of residues that contribute to the salt bridge network at the PDZ/protease domain interface increase levels of basal σ^E activity but do not further enhance activation in the presence of stress beyond that of wild-type DegS (50). We suggest that the disruption of the local network of salt bridges at the PDZ/protease domain interface in $DegS^{A323E}$ increases basal levels activation of $DegS^{A323E}$ but does not change the maximal activity of $DegS^{A323E}$ compared to that of wild-type DegS when stress is present.

Our work shows that $degS_{A323E}$ is a powerful suppressor of a number of distinct conditions that disrupt the outer membrane, including the $lamB_{G439D}$, $lptD_{Y721D}$, and Δ*bamB* Δ*bamE* mutations (Fig. 3 and 5). Other studies have also demonstrated that enhanced σ^E stress response signaling, resulting from *rpoE* mutants or *rseA* null mutations, can suppress numerous assembly-defective conditions (55, 56). We propose that $degS_{A323E}$ increases basal levels of σ^E signaling to prime the cell to respond to stress. Cell viability is ultimately determined by the race between escalating envelope stress and activation of stress response pathways. If left unchecked, the buildup of unfolded OMPs will reach toxic levels and kill the cell. Envelope stress response pathways detect unfolded OMP substrates and activate gene programs that counter the rapid accumulation of unfolded OMPs before they challenge cell viability. The increased levels of σ^E signaling exhibited by $degS_{A323E}$ prevent cell death by activating the protective σ^E regulon before the level of unfolded OMPs reaches lethal levels. Importantly, $degS_{A323E}$ lacks the growth defects characteristic of high levels of σ^E signaling (Fig. S3) (25–28, 54). Therefore, we suggest that $degS_{A323E}$ fine-tunes basal levels of σ^E activation to help the cell cope with stress associated with OMP assembly without creating the toxicity affiliated with high levels of σ^E activation.

MATERIALS AND METHODS

Bacterial strains and plasmids. All strains, plasmids, and oligonucleotides used in this study are presented in Table S1 in the supplemental material. All oligonucleotides were ordered from Integrated DNA Technologies. Strains were constructed using standard microbiological techniques and grown as previously described (60). When necessary, LB medium was supplemented with 20 mg/liter of chloramphenicol, 25 mg/liter of kanamycin (low), 50 mg/liter of kanamycin (high), 50 mg/liter of carbenicillin, or 10 mg/liter of tetracycline. Strains NovaBlue (Novagen), BL21(DE3) (Novagen), and Mach-1 (Thermo Fisher Scientific) were used for expression and cloning procedures. To evaluate suppression of the Δ*bamB* Δ*bamE* mutation, cultures were grown in M63 medium supplemented with 0.2% glucose, 1 mM $MgSO_4$, 100 μg/ml of thiamine, and a 500-μl volume of LB. Unless otherwise noted, all strains were grown and constructed at 30°C. Deletion alleles originated from the Keio Collection (28). In all strains, $degS_{A323E}$ was linked to the nearby *yhcG* Keio allele. Comparison of cells expressing $degS_{A323E}$ *yhcG*::*kan* was always made in reference to the isogenic control, which contained only *yhcG*::*kan*. When testing for suppression of the Δ*bamB* Δ*bamE* mutation, the *yhcG*::*kan* allele was removed by the use of FLP recombinase, as previously described (61). Growth phenotypes of wild-type, Δ*bamB*, Δ*bamE*, and Δ*bamB* Δ*bamE* strains were not altered by Δ*yhcG* (Fig. S4).

Western blot analysis. Overnight cultures were normalized by optical density at 600 nm (OD_{600}). Samples were resuspended in the same volume of sample buffer containing β-mercaptoethanol (β-ME). For oxidized blots, the sample buffer lacked β-ME. Samples were boiled for 10 min and subjected to electrophoresis through an SDS-PAGE gel (10% for LamB blots and 8% for LptD blots). Proteins were transferred to a nitrocellulose membrane (GE Healthcare, Amersham). Immunoblotting was performed using rabbit polyclonal antisera that recognize LamB/OmpA/MBP (1:25,000), trimeric LamB (1:16,500), LptD (1:25,000), and GroEL (1:10,000). Donkey anti-rabbit IgG–horseradish peroxidase secondary antibody (GE Healthcare) was used at 1:10,000 dilution for all immunoblots.

Trimeric LamB sample preparation. Overnight cultures were normalized by OD_{600}. Cells were resuspended in Bugbuster (Millipore), protease cocktail inhibitor (1:100; Sigma-Aldrich), benzonase (1:100; Sigma-Aldrich), and 1 M $MgCl_2$ (1:100). Samples were lysed for 10 min at room temperature. Laemmli sample buffer (Bio-Rad) supplemented with β-mercaptoethanol was added to dilute the sample volume 1:2. Samples were electrophoresed and analyzed as described above.

Preparation of biologically pure M63 minimal maltodextrin medium. M63 medium was supplemented with 80 ml/liter of maltodextrin solution, 1 mM $MgSO_4$, and 100 μg/ml of thiamine. MG2930 was inoculated into the medium and grown overnight at 37°C. The cells were pelleted and the remaining supernatant was filtered (0.22-μm pore size; Millipore).

Growth phenotypes in minimal maltodextrin medium. Strains were grown under permissive conditions in LB or LB supplemented with 20 mg/liter of chloramphenicol, when appropriate. Cells were washed in M63 medium, and a normalized number of cells were inoculated into minimal maltodextrin

medium (containing 20 mg/liter of chloramphenicol for plasmid maintenance, when necessary). After 24 h of growth at 30°C, growth was scored.

Expression and purification of soluble BamD-His$_6$. Soluble BamD-His$_6$ was expressed from pCH86 in BL21(DE3) cells as described previously (41). Cultures were grown at 37°C to an OD_{600} of 0.4, and then protein expression was induced by adding 0.1 mM isopropyl-β-D-thiogalactopyranoside (IPTG). The cultures were incubated for another 3 to 4 h. The cells were collected by centrifugation at 5,000 × *g* and 4°C for 10 min and then resuspended in TBS (pH 8; defined as 20 mM Tris [pH 8] with 150 mM NaCl unless otherwise noted). They were lysed via cell disrupter and centrifuged again at 5,000 × *g* and 4°C for 10 min. Mechanical cell lysis was achieved using an EmulsiFlex-C3 cell disrupter (Avestin) at a pressure of 10,000 to 15,000 lb/in^2. The supernatant was collected and ultracentrifuged at 100,000 × *g* and 4°C for 30 min. The clarified supernatant was then subjected to nickel-nitrilotriacetic acid (Ni-NTA) affinity chromatography (Qiagen) followed by size exclusion chromatography (Superdex 200 column; GE Healthcare) in TBS (pH 8).

Expression and purification of wild-type and mutant LamB substrates and peptides. All full-length, truncated, and/or mutated forms of LamB were produced by expression in the cytoplasm of BL21(DE3) strains carrying the appropriate plasmid (pCH13, pJW384, pJW387, pJW410, pJW411, pJW412, pJW413, or pCH167). Cultures of these strains were grown at 37°C to an OD_{600} of 0.4. Expression of the proteins was then induced by addition of 0.1 mM IPTG, and the cultures were incubated for another 2 to 3 h. The cells were then harvested, resuspended in TBS (pH 8) with 0.1 mg/ml of DNase, 0.1 mg/ml of RNase, 0.1 mg/ml of lysozyme, and 1 mM phenylmethylsulfonyl fluoride (PMSF), and then lysed by cell disrupter. The cell lysates were centrifuged at 5,000 × *g* and 4°C for 10 min to pellet the inclusion bodies containing the LamB and BamA proteins or peptides. The inclusion bodies were washed once by resuspension in TBS (pH 8) and then centrifuged again at 5,000 × *g* and 4°C for 10 min. These inclusion bodies were dissolved in 8 M urea by incubation with rocking at 25°C for approximately 30 min. The solutions were then centrifuged at 18,000 × *g* and 4°C for 10 min to pellet any undissolved material. These clarified urea solutions contained only minor amounts of other contaminating proteins as judged by SDS-PAGE and were used in the subsequent assays without further purification.

Affinity purifications with LamB or BamA peptides and folded BamD-His. Urea-denatured peptides were normalized to a concentration of 1 mM in 8 M urea (all protein concentrations were determined using the Bio-Rad DC protein assay) and diluted 10-fold into a TBS solution containing BamD-His, such that final concentrations of 50 μM BamD-His and 100 μM peptide were achieved. These solutions were incubated at room temperature for 20 min, upon which time 10 μl was removed for "input samples." Eighty microliters of the remaining sample was applied to 200 μl of Ni-NTA slurry (preequilibrated with TBS–20 mM imidazole), and the resin was washed twice with 1 ml of TBS–20 mM imidazole. The residual protein was eluted with 600 μl of TBS–200 mM imidazole, and 70 μl of trichloroacetic acid was added to precipitate all protein components of the eluate. Following a 30-min incubation on ice, the samples were centrifuged at a relative centrifugal force (rcf) of 21,000 for 10 min. The resulting protein pellets were resuspended in 20 μl of 1 M Tris (pH 8) and diluted 1:1 with 2 × SDS sample buffer, and the samples were boiled for 5 min. Samples were analyzed via SDS-PAGE (200 V, 45 min, 4-μl input load, and 2.5-μl eluate load) followed by Coomassie staining.

Folding of wild-type or mutant LamB in detergent solution. Urea-denatured wild-type or mutant LamB was normalized to a concentration of 200 μM in 8 M urea and diluted 10-fold into 0.25% *n*-dodecyl-β-D-maltopyranoside (DDM; Anatrace)–20 mM Tris (pH 8). The resulting solutions were rocked at room temperature for 20 h. Samples were diluted 1:1 with 2× SDS sample buffer and boiled (or not) for 5 min. The resulting samples were analyzed via seminative SDS-PAGE (150 V, 2 h, 4°C, and 4-μl load).

Genetic linkage analysis. To quantitate selective pressure on deletion of *degP*, a *degP*::*kan* allele was introduced into strains by cotransduction with a nearby marker, *yadC*::Tn*10*. MC4100, BH191, BH290, and BH291 were infected with P1*vir* carrying both *degP*::*kan* and *yadC*::Tn*10* at 30°C and 37°C. Tet^r transductants were selected (and Cat^r, where applicable). These transductants were then screened for Kan^r. The ratio of Kan^r transductants to total transductants screened was used to calculate cotransduction frequency. Transduction frequencies are a result of 100 transductants screened each for three separate transductions.

Isolation of suppressor mutations. BH291 was grown at 30°C overnight in LB supplemented with 20 mg/liter of chloramphenicol. Overnight cultures were diluted and plated on MacConkey medium supplemented with 20 mg/liter of chloramphenicol and 60 ml/liter of maltodextrins. Plates were incubated overnight at 37°C. Colonies that were entirely red were streak purified onto MacConkey medium supplemented with chloramphenicol and maltodextrins to ensure maintenance of the red growth phenotype. The background of the isolated suppressor was confirmed by colony PCR for *lamB* deletion and *degP* deletion, as well as cell death at 42°C to confirm *degP* deletion (62). The plasmid from the suppressor was isolated using the QIAprep spin miniprep kit (Qiagen) and sequenced using Sanger sequencing (Genewiz Inc.) to screen for potential revertants. Finally, the suppressor plasmid was transformed into a clean background (BH273) to determine if the suppression was plasmid linked or chromosomal. Only chromosomal suppressors were pursued. The $degS_{A323E}$ suppressor mutation described here was linked to a nearby genetic marker, *yhcG*::*kan* (28). This allowed the $degS_{A323E}$ allele to be moved into different strains by transduction, as previously described (60).

Whole-genome sequencing sample preparation. A genomic DNA sample of KT26 was isolated using the DNeasy blood and tissue kit (Qiagen), according to the manufacturer protocol described for Gram-negative organisms. An Illumina (CA) sequencing library of the genomic sample was prepared using the Nextera DNA library prep kit. The library was sequenced on an Illumina HiSeq 2500 sequencer with 75-nucleotide end reads in accordance with the standard manufacturer protocol.

Whole-genome sequencing analysis. Demultiplexed reads were assembled using the SPAdes genome assembly algorithm (63). The assembled genome was then aligned to a reference genome (*Escherichia coli* K-12; GenBank accession number NC_000913.3) using the Mauve multiple-genome-alignment program (64, 65). Nucleotide changes in the suppressor genome (KT26) relative to the reference genome were identified, and mutations were confirmed by Sanger sequencing of PCR-amplified loci (Genewiz Inc.).

***β*-Galactosidase assay.** Overnight cultures were diluted 1:100 in fresh LB and grown until late exponential phase (OD_{600} ~ 0.8 to 1.0). Samples were normalized by OD_{600}, pelleted, and resuspended in the same volume of Z buffer (60 mM Na_2HPO_4, 40 mM NaH_2PO_4, 10 mM KCl, 1 mM $MgSO_4$, 50 mM β-ME). Thirty microliters of 0.1% SDS and a 50-μl volume of chloroform were added. Samples were vortexed for 10 s each and left to lyse for 10 min. A 100-μl volume of each cell lysate was mixed with 50 μl of 4-mg/ml *O*-nitrophenyl-β-D-galactopyranoside (ONPG) solution in Z buffer. β-Galactosidase activity was analyzed by kinetic measurement of OD_{420} in a BioTek Synergy H1 plate reader, and V_{max} was determined using Gen5 software. Experiments were performed in three biological replicates, and mean values ± standard errors of the means (SEM) were plotted. Significance was determined by a *t* test.

Efficiency-of-plating (EOP) assay. Overnight cultures were normalized by OD_{600}. For assaying Δ*bamB* Δ*bamE* cell viability, 10-fold dilutions were made in minimal glucose, replica plated onto LB or minimal glucose plates, and incubated at 30°C and 37°C.

Growth curves. Overnight cultures were normalized by OD_{600}. Cells were inoculated into 2 ml of fresh LB in a 24-well microtiter plate (Corning no. 3526). Cultures were grown at 37°C with aeration in a BioTek Synergy H1 plate reader for 16 h. Growth curves were performed in biological triplicate and mean values ± standard deviations were plotted.

SUPPLEMENTAL MATERIAL

Supplemental material for this article may be found at https://doi.org/10.1128/JB.00745-18.

SUPPLEMENTAL FILE 1, PDF file, 5.9 MB.

ACKNOWLEDGMENTS

We thank current and former members of the T.J.S. and D.K. laboratories for helpful discussion and Wei Wang and Jessica Wiggins at the Lewis-Sigler Institute Genomics Core Facility of Princeton University for performing the whole-genome sequencing. We also thank Rajeev Misra for sharing unpublished data and productive conversation.

Research reported in this publication was supported by the National Institute of General Medicine Sciences of the National Institutes of Health under grant no. R35-GM118024 and R01-GM034821 (to T.J.S.) and grant no. T32-GM007388 (to Princeton University [E.M.H.]) and the National Institute of Allergy and Infectious Disease of the National Institutes of Health under grant no. R01-AI081059 (to D.K.).

The content of this publication is solely the responsibility of the authors and does not necessarily represent the official views of the National Institutes of Health.

E.M.H., A.O., J.S.W., D.K., and T.J.S. designed the research. E.M.H, K.T., M.G., and J.S.W. performed the research. E.M.H. and T.J.S. wrote the paper.

REFERENCES

1. Silhavy TJ, Kahne D, Walker S. 2010. The bacterial cell envelope. Cold Spring Harb Perspect Biol 2:a000414. https://doi.org/10.1101/cshperspect.a000414.
2. Nikaido H, Vaara M. 1992. Molecular basis of bacterial outer membrane permeability. Microbiol Rev 49:1–32.
3. Du Plessis DJ, Nouwen N, Driessen AJ. 2011. The Sec translocase. Biochim Biophys Acta 1808:851–865. https://doi.org/10.1016/j.bbamem.2010.08.016.
4. Beckwith J. 2013. The Sec-dependent pathway. Res Microbiol 164:497–504. https://doi.org/10.1016/j.resmic.2013.03.007.
5. Hagan CL, Silhavy TJ, Kahne D. 2011. β-Barrel membrane protein assembly by the Bam complex. Annu Rev Biochem 80:189–210. https://doi.org/10.1146/annurev-biochem-061408-144611.
6. Konovalova A, Kahne D, Silhavy TJ. 2017. Outer membrane biogenesis. Annu Rev Microbiol 71:539–556. https://doi.org/10.1146/annurev-micro-090816-093754.
7. Merdanovic M, Clausen T, Kaiser M, Huber R, Ehrmann M. 2011. Protein quality control in the bacterial periplasm. Annu Rev Microbiol 65:149–168. https://doi.org/10.1146/annurev-micro-090110-102925.
8. Konovalova A, Grabowicz M, Balibar CJ, Malinverni JC, Painter RE, Riley D, Mann PA, Wang H, Garlisi CG, Sherborne B, Rigel NW, Ricci DP, Black TA, Roemer T, Silhavy TJ, Walker SS. 2018. Inhibitor of intramembrane protease RseP blocks the σ^E response causing lethal accumulation of unfolded outer membrane proteins. Proc Natl Acad Sci U S A 15:E6614–E6621. https://doi.org/10.1073/pnas.1806107115.
9. Ades SE. 2008. Regulation by destruction: design of the σ^E envelope stress response. Curr Opin Microbiol 11:535–540. https://doi.org/10.1016/j.mib.2008.10.004.
10. Barchinger SE, Ades SE. 2013. Regulated proteolysis: control of the *Escherichia coli* σ^E-dependent cell envelope stress response, p 129–160. *In* Dougan DA (ed), Regulated proteolysis in microorganisms. Springer Netherlands, Dordrecht, The Netherlands.
11. Struyve M, Moons M, Tommassen J. 1991. Carboxy-terminal phenylalanine is essential for the correct assembly of a bacterial outer membrane protein. J Mol Biol 218:141–148. https://doi.org/10.1016/0022-2836(91)90880-F.
12. Alba BM, Zhong HJ, Pelayo JC, Gross CA. 2001. *degS* (*hhoB*) is an essential *Escherichia coli* gene whose indispensable function is to provide σ^E activity. Mol Microbiol 40:1323–1333. https://doi.org/10.1046/j.1365-2958.2001.02475.x.
13. Walsh NP, Alba BM, Bose B, Gross CA, Sauer RT. 2003. OMP peptide signals initiate the envelope-stress response by activating DegS protease via relief of inhibition mediated by its PDZ domain. Cell 113:61–71. https://doi.org/10.1016/S0092-8674(03)00203-4.

14. Alba BM, Leeds JA, Onufryk C, Lu CZ, Gross CA. 2002. DegS and YaeL participate sequentially in the cleavage of RseA to activate the sigma E-dependent extracytoplasmic stress response. Genes Dev 16:2156–2168. https://doi.org/10.1101/gad.1008902.
15. Kanehara K, Ito K, Akiyama Y. 2002. YaeL (EcfE) activates the σ^E pathway of stress response through a site-2 cleavage of anti-σ^E, RseA. Genes Dev 16:2147–2155. https://doi.org/10.1101/gad.1002302.
16. Kanehara K, Ito K, Akiyama Y. 2003. YaeL proteolysis of RseA is controlled by the PDZ domain of YaeL and a Gln-rich region of RseA. EMBO 22:6839–6398.
17. Akiyama Y, Kanehara K, Ito K. 2004. RseP (YaeL), an Escherichia coli RIP protease, cleaves transmembrane sequences. EMBO J 23:4434–4442. https://doi.org/10.1038/sj.emboj.7600449.
18. Flynn JM, Levchenko I, Sauer RT, Baker TA. 2004. Modulating substrate choice: the SspB adaptor delivers a regulator of the extracytoplasmic-stress response to the AAA+ protease ClpXP for degradation. Genes Dev 18:2292–2301. https://doi.org/10.1101/gad.1240104.
19. Missiakas D, Mayer MP, Lemaire M, Georgopoulos C, Raina S. 1997. Modulation of the *Escherichia coli* σ^E (RpoE) heat-shock transcription-factor activity by the RseA, RseB, and RseC proteins. Mol Microbiol 24:355–371. https://doi.org/10.1046/j.1365-2958.1997.3601713.x.
20. Ades SE, Connolly LE, Alba BM, Gross CA. 1999. The *Escherichia coli* σ^E-dependent extracytoplasmic stress response is controlled by the regulated proteolysis of an anti-σ factor. Genes Dev 13:2449–2461. https://doi.org/10.1101/gad.13.18.2449.
21. Rhodius VA, Suh WC, Nonaka G, West J, Gross CA. 2006. Conserved and variable functions of the σ^E stress response in related genomes. PLoS Biol 4:e2–17. https://doi.org/10.1371/journal.pbio.0040002.
22. Johansen J, Rasmussen AA, Overgaard M, Valentin-Hansen P. 2006. Conserved small non-coding RNAs that belong to the σ^E regulon: role in down-regulation of outer membrane proteins. J Mol Biol 364:1–8. https://doi.org/10.1016/j.jmb.2006.09.004.
23. Las Peñas de A, Connolly L, Gross CA. 1997. σE is an essential sigma factor in *Escherichia coli*. J Bacteriol 179:6862–6864. https://doi.org/10.1128/jb.179.21.6862-6864.1997.
24. Hayden JD, Ades SE. 2008. The extracytoplasmic stress factor, σ^E, is required to maintain cell envelope integrity in *Escherichia coli*. PLoS One 3:e1573. https://doi.org/10.1371/journal.pone.0001573.
25. Nitta T, Nagamitsu H, Murata M, Izu H, Yamada M. 2000. Function of the σ^E regulon in dead-cell lysis in stationary-phase *Escherichia coli*. J Bacteriol 182:5231–5237. https://doi.org/10.1128/JB.182.18.5231-5237.2000.
26. Noor R, Murata M, Nagamitsu H, Klein G, Raina S, Yamada M. 2009. Dissection of σ^E-dependent cell lysis in *Escherichia coli*: roles of RpoE regulators RseA, RseB and periplasmic folding catalyst PpiD. Genes Cells 14:885–899. https://doi.org/10.1111/j.1365-2443.2009.01318.x.
27. Kabir MS, Yamashita D, Koyama S, Oshima T, Kurokawa K, Maeda M, Tsunedomi R, Murata M, Wada C, Mori H, Yamada M. 2005. Cell lysis directed by σ^E in early stationary phase and effect of induction of the *rpoE* gene on global gene expression in *Escherichia coli*. Microbiology 151:2721–2735. https://doi.org/10.1099/mic.0.28004-0.
28. Baba T, Ara T, Hasegawa M, Takai Y, Okumura Y, Baba M, Datsenko KA, Tomita M, Wanner BL, Mori H. 2006. Construction of *Escherichia coli* K-12 in-frame, single-gene knockout mutants: the Keio collection. Mol Syst Biol 2:473–411.
29. Ades SE, Grigorova IL, Gross CA. 2003. Regulation of the alternative sigma factor σ^E during initiation, adaptation, and shutoff of the extracytoplasmic heat shock response in *Escherichia coli*. J Bacteriol 185:2512–2519. https://doi.org/10.1128/JB.185.8.2512-2519.2003.
30. Li G-W, Burkhardt D, Gross C, Weissman JS. 2014. Quantifying absolute protein synthesis rates reveals principles underlying allocation of cellular resources. Cell 157:624–635. https://doi.org/10.1016/j.cell.2014.02.033.
31. Szmelcman S, Hofnung M. 1975. Maltose transport in *Escherichia coli* K-12: involvement of the bacteriophage lambda receptor. J Bacteriol 124:112–118.
32. Wang Y-F, Dutzler R, Rizkallah PJ, Rosenbusch JP, Schirmer T. 1997. Channel specificity: structural basis for sugar discrimination and differential flux rates in maltoporin. J Mol Biol 272:56–63. https://doi.org/10.1006/jmbi.1997.1224.
33. Cole ST, Raibaud O. 1986. The nucleotide sequence of the *malT* gene encoding the positive regulator of the *Escherichia coli* maltose regulon. Gene 42:201–208. https://doi.org/10.1016/0378-1119(86)90297-0.
34. Raibaud O, Vidal-Ingigliardi D, Richet E. 1989. A complex nucleoprotein structure involved in activation of transcription of two divergent *Escherichia coli* promoters. J Mol Biol 205:471–485. https://doi.org/10.1016/0022-2836(89)90218-0.
35. Robert V, Volokhina EB, Senf F, Bos MP, Van Gelder P, Tommassen J. 2006. Assembly factor Omp85 recognizes its outer membrane protein substrates by a species-specific C-terminal motif. PLoS Biol 4:e377. https://doi.org/10.1371/journal.pbio.0040377.
36. Kutik S, Stojanovski D, Becker L, Becker T, Meinecke M, Krüger V, Prinz C, Meisinger C, Guiard B, Wagner R, Pfanner N, Wiedemann N. 2008. Dissecting membrane insertion of mitochondrial β-barrel proteins. Cell 132:1011–1024. https://doi.org/10.1016/j.cell.2008.01.028.
37. Hagan CL, Wzorek JS, Kahne D. 2015. Inhibition of the β-barrel assembly machine by a peptide that binds BamD. Proc Natl Acad Sci U S A 112:2011–2016. https://doi.org/10.1073/pnas.1415955112.
38. Wzorek JS, Lee J, Tomasek D, Hagan CL, Kahne D. 2017. Membrane integration of an essential β-barrel protein prerequires burial of an extracellular loop. Proc Natl Acad Sci U S A 114:2598–2603. https://doi.org/10.1073/pnas.1616576114.
39. Lee J, Xue M, Wzorek JS, Wu T, Grabowicz M, Gronenberg LS, Sutterlin HA, Davis RM, Ruiz N, Silhavy TJ, Kahne D. 2016. Characterization of a stalled complex on the β-barrel assembly machine. Proc Natl Acad Sci U S A 113:8717–8722. https://doi.org/10.1073/pnas.1604100113.
40. Lee J, Sutterlin HA, Wzorek JS, Mandler MD, Hagan CL, Grabowicz M, Tomasek D, May MD, Hart EM, Silhavy TJ, Kahne D. 2018. Substrate binding to BamD triggers a conformational change in BamA to control membrane insertion. Proc Natl Acad Sci U S A 115:2359–2364. https://doi.org/10.1073/pnas.1711727115.
41. Hagan CL, Westwood DB, Kahne D. 2013. Bam lipoproteins assemble BamA in vitro. Biochemistry 52:6108–6113. https://doi.org/10.1021/bi400865z.
42. Noinaj N, Kuszak AJ, Buchanan SK. 2015. Heat modifiability of outer membrane proteins from Gram-negative bacteria. Methods Mol Biol 1329:51–56. https://doi.org/10.1007/978-1-4939-2871-2_4.
43. Soltes GR, Martin NR, Park E, Sutterlin HA, Silhavy TJ. 2017. Distinctive roles for periplasmic proteases in the maintenance of essential outer membrane protein assembly. J Bacteriol 199:e00418-17. https://doi.org/10.1128/JB.00418-17.
44. Speiss C, Beil A, Ehrmann M. 1999. A temperature-dependent switch from chaperone to protease in a widely conserved heat shock protein. Cell 971:339–3479. https://doi.org/10.1016/S0092-8674(00)80743-6.
45. Shuman HA, Silhavy TJ. 2003. The art and design of genetic screens: *Escherichia coli*. Nat Rev Genet 4:419–431. https://doi.org/10.1038/nrg1087.
46. Mauldin RV, Sauer RT. 2013. Allosteric regulation of DegS protease subunits through a shared energy landscape. Nat Chem Biol 9:90–96. https://doi.org/10.1038/nchembio.1135.
47. Sohn J, Sauer RT. 2009. OMP peptides modulate the activity of DegS protease by differential binding to active and inactive conformations. Mol Cell 33:64–74. https://doi.org/10.1016/j.molcel.2008.12.017.
48. Wilken C, Kitzing K, Kurzbauer R, Ehrmann M, Clausen T. 2004. Crystal structure of the DegS stress sensor: how a PDZ domain recognizes misfolded protein and activates a protease. Cell 117:483–494. https://doi.org/10.1016/S0092-8674(04)00454-4.
49. Zeth K. 2004. Structural analysis of DegS, a stress sensor of the bacterial periplasm. FEBS Lett 569:351–358. https://doi.org/10.1016/j.febslet.2004.06.012.
50. Sohn J, Grant RA, Sauer RT. 2007. Allosteric activation of DegS, a stress sensor PDZ protease. Cell 131:572–583. https://doi.org/10.1016/j.cell.2007.08.044.
51. Button JE, Silhavy TJ, Ruiz N. 2007. A suppressor of cell death caused by the loss of σ^E downregulates extracytoplasmic stress responses and outer membrane vesicle production in *Escherichia coli*. J Bacteriol 189:1523–1530. https://doi.org/10.1128/JB.01534-06.
52. Missiakas D, Betton J-M, Raina S. 1996. New components of protein folding in extracytoplasmic compartments of *Escherichia coli* SurA, FkpA and Skp/OmpH. Mol Microbiol 21:871–884. https://doi.org/10.1046/j.1365-2958.1996.561412.x.
53. Rouvière PE, Gross CA. 1996. SurA, a periplasmic protein with peptidyl-prolyl isomerase activity, participates in the assembly of outer membrane porins. Genes Dev 10:3170–3182. https://doi.org/10.1101/gad.10.24.3170.
54. Nicoloff H, Gopalkrishnan S, Ades SE. 2017. Appropriate regulation of the σ^E-dependent envelope stress response is necessary to maintain cell envelope integrity and stationary-phase survival in *Escherichia coli*. J Bacteriol 199:203–217.

55. Leiser OP, Charlson ES, Gerken H, Misra R. 2012. Reversal of the Δ*degP* phenotypes by a novel *rpoE* allele of *Escherichia coli*. PLoS One 7:e33979. https://doi.org/10.1371/journal.pone.0033979.
56. Konovalova A, Schwalm JA, Silhavy TJ. 2016. A suppressor mutation that creates a faster and more robust σ^e envelope stress response. J Bacteriol 198:2345–2351. https://doi.org/10.1128/JB.00340-16.
57. Sklar JG, Wu T, Gronenberg LG, Malinverni JC, Malinverni J, Kahne D, Silhavy TJ. 2007. Lipoprotein SmpA is a component of the YaeT complex that assembles outer membrane proteins in *Escherichia coli*. Proc Natl Acad Sci U S A 104:6400–6405. https://doi.org/10.1073/pnas.0701579104.
58. Tellez R, Misra R. 2012. Substitutions in the BamA β-barrel domain overcome the conditional lethal phenotype of a Δ*bamB bamE* Strain of *Escherichia coli*. J Bacteriol 194:317–324. https://doi.org/10.1128/JB.06192-11.
59. de Regt AK, Baker TA, Sauer RT. 2015. Steric clashes with bound OMP peptides activate the DegS stress-response protease. Proc Natl Acad Sci U S A 112:3326–3331. https://doi.org/10.1073/pnas.1502372112.
60. Silhavy TJ, Berman ML, Enquist LW. 1984. Experiments with gene fusions. Cold Spring Harbor Laboratory Press, Cold Spring Harbor, NY.
61. Datsenko KA, Wanner BL. 2000. One-step inactivation of chromosomal genes in *Escherichia coli* K-12 using PCR products. Proc Natl Acad Sci U S A 97:6640–6645. https://doi.org/10.1073/pnas.120163297.
62. Lipinska B, Zylicz M, Georgopoulos C. 1990. The HtrA (DegP) protein, essential for *Escherichia coli* survival at high temperatures, is an endopeptidase. J Bacteriol 172:1791–1797. https://doi.org/10.1128/jb.172.4.1791-1797.1990.
63. Bankevich A, Nurk S, Antipov D, Gurevich AA, Dvorkin M, Kulikov AS, Lesin VM, Nikolenko SI, Pham S, Prjibelski AD, Pyshkin AV, Sirotkin AV, Vyahhi N, Tesler G, Alekseyev MA, Pevzner PA. 2012. SPAdes: a new genome assembly algorithm and its applications to single-cell sequencing. J Comput Biol 19:455–477. https://doi.org/10.1089/cmb.2012.0021.
64. Darling AC, Mau B, Blattner FR, Perna NT. 2004. Mauve: multiple alignment of conserved genomic sequence with rearrangements. Genome Res 14:1394–1403. https://doi.org/10.1101/gr.2289704.
65. Edwards DJ, Holt KE. 2013. Beginner's guide to comparative bacterial genome analysis using next-generation sequence data. Microb Inform Exp 3:2. https://doi.org/10.1186/2042-5783-3-2.